Role of the Jahn-Teller effect of the V^{2+} center in the magnetic anisotropy of $Cd_{1-x}V_xS$ and $Cd_{1-x}V_xSe$

M. Herbich, W. Mac, and A. Twardowski
Institute of Experimental Physics, Warsaw University, Hoża 69, 00-681 Warsaw, Poland

M. Demianiuk
Institute of Technical Physics, Military Academy of Technology, 00-908 Warsaw, Poland

(Received 29 June 1998)

The magnetization measurements of the wurtzite crystals $Cd_{1-x}V_xS$ and $Cd_{1-x}V_xSe$ for magnetic field (up to 6 T) parallel and perpendicular to the crystal hexagonal axis are presented. Strong anisotropy of magnetization is observed for $Cd_{1-x}V_xS$ at low temperatures (2, 10 K), while for $Cd_{1-x}V_xSe$ the anisotropy is much weaker. The magnetization data are well described by the crystal-field model of the V^{2+} center, taking into account strong static Jahn-Teller effect of the trigonal symmetry. The differences in the anisotropy of magnetization for $Cd_{1-x}V_xS$ and $Cd_{1-x}V_xSe$ are interpreted as due to the different distributions of different V^{2+} centers for both systems. [S0163-1829(99)15103-8]

I. INTRODUCTION

Diluted magnetic semiconductors[1] (DMS's) with transition-metal ions with less than half-filled *d* shell (Cr, V, Ti, Sc) are of particular interest due to the ferromagnetic character of the *p-d* exchange interaction predicted by the theory[2,3] and confirmed experimentally for Cr-based DMS's.[4,5] Moreover, in contrast with Mn-, Co-, and Fe-based DMS's the proper description of the localized spins in the DMS's based on Cr^{2+} or V^{2+} ions must take into account a strong static Jahn-Teller effect of the magnetic ion (tetragonal in the case of chromium,[6–9] trigonal in the case of vanadium[11]). In the particular case of Cr-based DMS's, there are three types of Cr^{2+} centers distorted along the $\langle 100\rangle$ axes. These Jahn-Teller distortion axes were found to be easy axes for the Cr^{2+} spin, so, recalling that, in the wurtzite crystals, they are equivalent with respect to the hexagonal *c* axis, none of the Cr^{2+} types of centers are privileged in the magnetic field applied along the *c* axis.

In the case of vanadium-based DMS's the situation is different. V^{2+} ion ($L=3, S=\frac{3}{2}$) suffers Jahn-Teller effect along with one of the four $\langle 111\rangle$ axes in cubic coordinates. The hexagonal *c* axis of the wurtzite crystals is often regarded as one of the possible $\langle 111\rangle$ cubic directions. In such considerations, one of the V^{2+} Jahn-Teller distortion axes coincides with the *c* axis. The centers distorted along the *c* axis are, therefore, distinguished from the others and therefore can be populated differently than the others. Generally, the population may depend on the strength of the hexagonal crystal field and spin-orbit coupling. Therefore, we found it worthwhile to study the problem of V^{2+} in two wurtzite materials, CdS and CdSe, in some detail.

In this paper we present magnetization study of $Cd_{1-x}V_xS$ and $Cd_{1-x}V_xSe$. We develop the crystal-field model of the V^{2+} center in these materials, and we interpret the experimental data within this model.

II. EXPERIMENT

The $Cd_{1-x}V_xS$($Cd_{1-x}V_xSe$) crystals were grown from CdS (CdSe) and V powders by the modified Bridgman technique, at the Institute of Technical Physics, Military Academy of Technology (Warsaw). Single-phase crystals were obtained only for rather low vanadium concentrations (*x* below 0.0005). Since standard methods used to determine crystal composition (atomic absorption or wet chemical analysis) are rather inaccurate for such low *x* values, the vanadium content was estimated from the magnetization data (see below). The measurements were performed using a superconducting quantum interference device.

Magnetization (per unit mass) was measured on oriented samples, with magnetic field parallel or perpendicular to the crystal hexagonal axis ($\mathbf{B}\|c$ or $\mathbf{B}\perp c$). Figure 1 shows the results obtained at $T=2.0$ K for $Cd_{1-x}V_xS$ and $Cd_{1-x}V_xSe$ samples. The low concentration of vanadium in these crystals results in paramagnetic contribution to the total magnetization being comparable to the diamagnetic part. This also means that, for these concentrations, more than 97% of V^{2+} ions have no nearest-magnetic neighbors, so *d-d* exchange, if any, can be neglected. Therefore, the model that assumes a system of noninteracting V^{2+} ions should provide a reasonable description.[8]

The anisotropy of the magnetization for $\mathbf{B}\|c$ and $\mathbf{B}\perp c$ is clearly visible. Since the diamagnetic contribution of the host lattices is isotropic the entire anisotropy results from the paramagnetic contribution for both $Cd_{1-x}V_xS$ and $Cd_{1-x}V_xSe$. The magnitude of the magnetization is larger for $\mathbf{B}\|c$ than for $\mathbf{B}\perp c$, which is more pronounced for $Cd_{1-x}V_xS$.

III. THEORY

The magnetization per unit mass is, for the system of noninteracting magnetic ions, the product of the mean magnetic moment of an ion and the number of the ions in the crystal

$$\mathbf{M}=-\frac{\mu_B}{m_{\text{molec}}}x\langle\hat{\mathbf{L}}+2\hat{\mathbf{S}}\rangle, \tag{1}$$

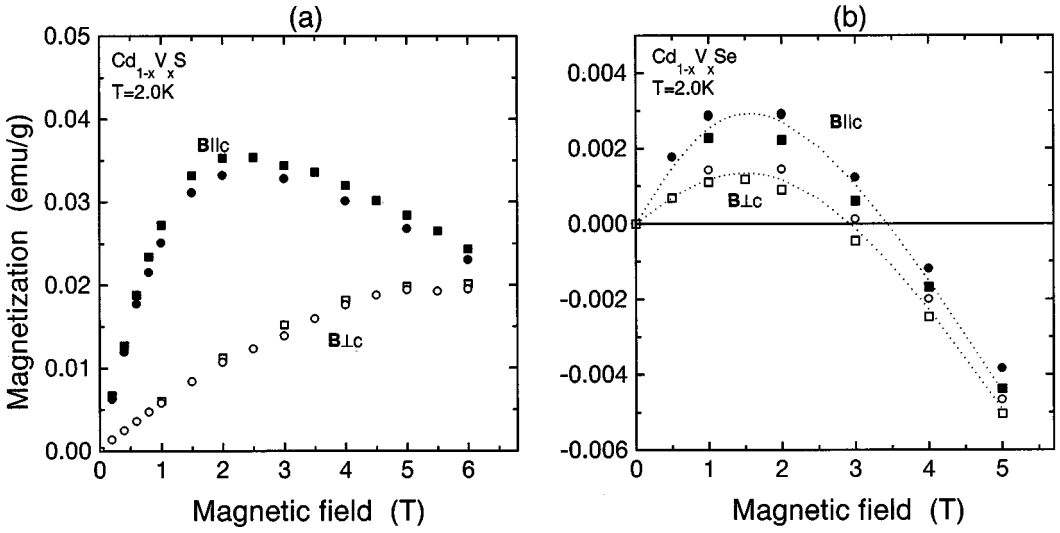

FIG. 1. Magnetization of two samples (circles and squares) of $Cd_{1-x}V_xS$ (left-hand side) and two samples of $Cd_{1-x}V_xSe$ (right-hand side) at $T=2.0$ K. The magnetic field was applied parallel (full points) or perpendicular (open points) to the crystallographic c axis. The dotted lines are guides to the eye only. The data are *not* corrected for the diamagnetism of the lattice.

where μ_B is the Bohr magneton, $m_{\text{molec}}=(1-x)m_{Cd}+xm_V+m_S$ is the mass of the $Cd_{1-x}V_xS$ ($Cd_{1-x}V_xSe$) ''molecule,'' x is the molar fraction of magnetic ions, and $-\langle\hat{\mathbf{L}}+2\hat{\mathbf{S}}\rangle$ is the mean magnetic moment of the V^{2+} ion. As already mentioned, the V^{2+} ion suffers strong static Jahn-Teller distortion along one of four $\langle 111\rangle$ axes. Therefore, four types of vanadium centers can be distinguished with respect to the hexagonal axis and given magnetic field $\mathbf{B}$: *A*, *B*, *C*, and *D* (let *A* be the type of center for which the Jahn-Teller distortion coincides with the c axis). In effect the mean magnetic moment $\langle\mathbf{M}\rangle=-\langle\mathbf{L}+2\mathbf{S}\rangle$ results from the averaging over these centers, which in total thermal equilibrium may be expressed as (compare Ref. 8)

$$\langle\mathbf{M}\rangle=\frac{1}{Z}(\alpha Z_A\langle\mathbf{M}\rangle_A+Z_B\langle\mathbf{M}\rangle_B+Z_C\langle\mathbf{M}\rangle_C+Z_D\langle\mathbf{M}\rangle_D), \tag{2}$$

where $Z_n(n=A,B,C,D)$ are the partition functions for each of the *A*, *B*, *C*, *D* centers at the given magnetic field: $Z_n=\Sigma_i\exp(-E_i^n/k_BT)$ (E_i^n are the eigenenergies of the nth center), $Z=\alpha Z_A+Z_B+Z_C+Z_D$, where α represents the difference in distribution of centers *A* with respect to *B*, *C*, and *D* due to hexagonal distortion (there is α times more *A* centers than any other). For $\mathbf{B}\|c$ we can reduce the problem of four types of centers to two types, since center *A* coincides with the hexagonal stress and three others, *B*, *C*, and *D*, are equivalent with respect to the c axis. For $\mathbf{B}\perp c$ the problem, in principle, involves all four different types of centers (discussed below).

Let $\langle\mathbf{M}_n\rangle$ be the thermodynamic average of the operator $\hat{\mathbf{M}}=-(\hat{\mathbf{L}}+2\hat{\mathbf{S}})$ for the center n:

$$\langle\mathbf{M}_n\rangle=\frac{\sum_{i=1}^{N}-\langle\varphi_i^n|\hat{\mathbf{L}}+2\hat{\mathbf{S}}|\varphi_i^n\rangle\exp\left(\frac{-E_i^n}{k_BT}\right)}{\sum_{i=1}^{N}\exp\left(\frac{-E_i^n}{k_BT}\right)}, \tag{3}$$

where k_B is the Boltzmann constant and the index i refers to the ith eigenstate φ_i of the energy E_i of the V^{2+} ion. Evaluation of $\langle M\rangle$ can be done after the eigenproblem of a certain V^{2+} center is solved. To do this we started from the Hamiltonian describing the effect of the crystal field,

$$\mathcal{H}=\mathcal{H}_{cf}+\mathcal{H}_{JT}+\mathcal{H}_{SO}+\mathcal{H}_B, \tag{4}$$

where $\mathcal{H}_{cf}$ is the cubic crystal field of (T_d symmetry), $\mathcal{H}_{JT}$ is the Jahn-Teller distortion of trigonal symmetry along one of four $\langle 111\rangle$ axes, $\mathcal{H}_{SO}$ is the spin-orbit coupling, and $\mathcal{H}_B$ represents the direct Zeeman interaction of the V^{2+} ion with magnetic field. Equation (4) should formally include the hexagonal crystal field; however, this correction is about two orders of magnitude smaller than $\mathcal{H}_{JT}$. We recall that the only change yielded by the hexagonal crystal field to the energy structure of the Jahn-Teller distorted center of the Cr^{2+} ion in CdS was that the first excited doublet became a semidoublet split by about 1% of the splitting between the ground and the first excited state.[10] For the V^{2+} ion we have no information about the strength of the hexagonal crystal field affecting the V^{2+} ion. However, if it is of the same order of magnitude as the Cr^{2+} ion, it can be neglected for the discussion below. This is due to the fact that the Jahn-Teller effect is predominantly stronger than the hexagonal crystal field, and therefore it forces its distortion axis. On the other hand, if the Jahn-Teller distortion axis coincides with the c axis (center *A*), then Hamiltonian (4) becomes strict (both $\mathcal{H}_{JT}$ and hexagonal crystal field have trigonal symmetry).[12,13]

The expressions for the crystal field Hamiltonians in terms of Stevens equivalent operators are[14]

$$\mathcal{H}_{cf}=-\frac{2}{3}B_4(\hat{O}_4^0-20\sqrt{2}\hat{O}_4^3), \tag{5a}$$

$$\mathcal{H}_{JT}=B_2^0\hat{O}_2^0+B_4^0\hat{O}_4^0, \tag{5b}$$

where $\hat{O}$ are the Stevens operators and B_l^k are parameters.

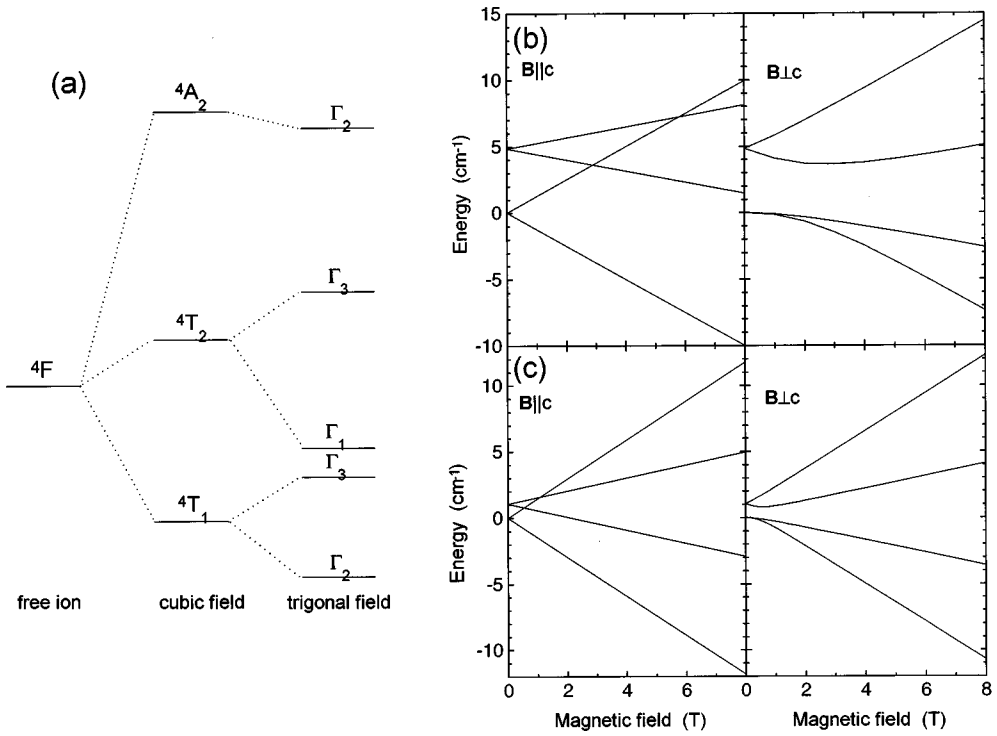

FIG. 2. Calculated energy diagram of the V^{2+} center: (a) the orbital terms, (b) and (c) the spin levels in the magnetic field ($\mathbf{B}||c$ on the left-hand side, $\mathbf{B}\perp c$ on the right-hand side) for two different spin-orbit parameters—(b) $\lambda=40\ \mathrm{cm}^{-1}$ and (c) $\lambda=-20\ \mathrm{cm}^{-1}$. The Jahn-Teller distortion axis was assumed collinear with the c axis (type A).

The first term of Hamiltonian (4), $\mathcal{H}_{\mathrm{cf}}$, splits the free ion ground term ($^4F, L=3, S=\frac{3}{2}$) into another orbital triplet $^4T_1$, which becomes the ground state, an orbital triplet $^4T_2$ (the first excited state), and an orbital singlet $^4A_2$ (see Fig. 2). The splitting between the $^4T_2$ level and $^4A_2$, $600B_4=10Dq$ ($10Dq$ denotes the cubic field splitting for a single d electron), is of the order of $4000\ \mathrm{cm}^{-1}$ for both V^{2+} in CdS and CdSe (Refs. 15 and 16). We note that the exact value is not crucial here, since our interest will be focused on the lowest-spin sublevels that determine the magnetization at low temperatures. The triplet $^4T_2$ is located $480B_4=8Dq$ higher than $^4T_1$, making the overall ^4F splitting equal to $18Dq$. The trigonal field splits the $^4T_1$ term into an orbital singlet $^4\Gamma_2$ (ground) and an orbital doublet $^4\Gamma_3$ located $4.5B_2^0+600B_4^0$ higher. The spin-orbit coupling, $\mathcal{H}_{\mathrm{SO}}=\lambda\cdot\hat{\mathbf{L}}\cdot\hat{\mathbf{S}}$, splits the ground state $^4\Gamma_2$ into two spin doublets [Figs. 2(b) and 2(c)]. Finally, the magnetic field, described by the Zeeman term $\mathcal{H}_B=\mu_{\mathrm{B}}(\hat{\mathbf{L}}+2\hat{\mathbf{S}})\cdot\mathbf{B}$, lifts all of the remaining degeneracies. We note that different centers A, B, C, or D differ by orientation of magnetic field $\mathbf{B}$ relative to the Jahn-Teller distortion.

As a basis for this eigenproblem we used the set of 28 wave functions described by L and S quantum numbers. The eigenenergies, as well as eigenstates, were then obtained strictly by the full diagonalization of a 28×28 Hamiltonian matrix. The cubic crystal-field parameter Dq used for the calculations was assumed the same for both CdS and CdSe: $Dq=420\ \mathrm{cm}^{-1}$, which corresponds to $B_4=7\ \mathrm{cm}^{-1}$. In order to describe the observed anisotropy of magnetization in $Cd_{1-x}V_xS$ crystals (see Sec. III A) the following values of the Jahn-Teller parameters were used: $B_2^0=-112\ \mathrm{cm}^{-1}$ and $B_4^0=-1.87\ \mathrm{cm}^{-1}$. In fact, only a slight variation around both of these values allows us to obtain the proper curvature and the anisotropy of the experimental data (however, there is some correlation between these parameters—a quite reasonable description may be obtained using B_4^0 between $-1.6\ \mathrm{cm}^{-1}$ and $-2.1\ \mathrm{cm}^{-1}$, while, simultaneously, the value of B_2^0 has to vary from $-115\ \mathrm{cm}^{-1}$ to $-110\ \mathrm{cm}^{-1}$). The strength of the Jahn-Teller distortion was assumed the same in CdS and CdSe. The spin-orbit coupling parameter $\lambda=40\ \mathrm{cm}^{-1}$ was estimated from the EPR studies of ZnS:V,[11] assuming that V^{2+} in CdS does not differ dramatically from that of ZnS (similarly to the situation for the Cr^{2+} ion[5,12]). In effect the spin-orbit splitting of the ground level Γ_2 is equal to $4.04\ \mathrm{cm}^{-1}$.

The paramagnetic contribution to the magnetization was then calculated using the expressions (2) and (3). The experimental magnetization data were corrected for the diamagnetic susceptibility of the host lattice:[17] $\chi^{\mathrm{d}}_{\mathrm{CdS}}=-3.70\times10^{-7}$ emu/g, and $\chi^{\mathrm{d}}_{\mathrm{CdSe}}=-3.34\times10^{-7}$ emu/g, in order to be compared with the model. In Secs. III A and III B we separately discuss the situation for vanadium in CdS lattice and CdSe lattices. The vanadium concentrations were obtained from the fit of the model calculations to the experimental data using Eq. (1) for which x is the only free parameter. For $Cd_{1-x}V_xS$ samples, the molar fraction x does not vary being around 0.044%; for $Cd_{1-x}V_xSe$, $x\approx0.016\%$ for one sample and $x\approx0.017\%$ for the other.

A. Magnetization of $Cd_{1-x}V_xS$

Magnetization of $Cd_{1-x}V_xS$ at $T=2.0$ K, shown in Fig. 3, is strongly anisotropic—its magnitude for $\mathbf{B}\|c$ is about two times larger than for $\mathbf{B}\perp c$ at low fields ($B<3$ T). Assuming equal number of centers A, B, C, and D, we would

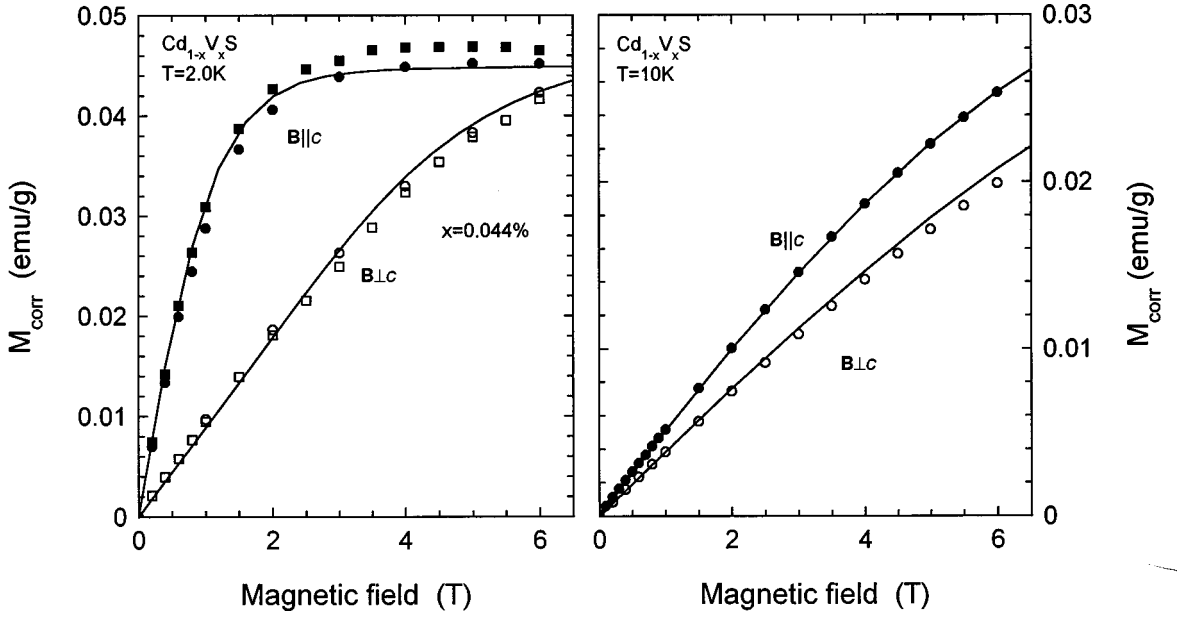

FIG. 3. Crystal-field model calculations of the magnetization curves (solid lines) for $Cd_{1-x}V_xS$ for two temperatures $T=2.0$ K (left-hand side) and $T=10$ K (right-hand side), according to the model assuming the Jahn-Teller distortion axis collinear with c axis for all V^{2+} ions. Points represent the experimental data, which were corrected for the diamagnetism of the CdS lattice $\chi^{d}_{CdS}=-3.70\times10^{-7}$ emu/g (Ref. 17) ($\mathbf{B}\|c$, full points; $\mathbf{B}\perp c$, empty points).

expect no anisotropy as the result of averaging over different centers. Thus the experimental observation suggests that the centers' distribution is not uniform. We recall that center A coincides with the c axis while for all the other centers (B,C, and D), distortion axes are tilted about 70.5° to the c axis. In effect centers B, C, and D are equivalent for $\mathbf{B}\|c$ and should be equally occupied. The difference between the occupation number for A center and the others results, obviously, in stronger anisotropy of the magnetization—Jahn-Teller distortion axis ''pins'' the spin as was already mentioned. Actually the best description of the experimental data is obtained if one assumes that only A centers are occupied. In other words, all the V^{2+} ions are distorted along the c axis (i.e., $\alpha\rightarrow\infty$). Magnetization calculated under this assumption is shown in Fig. 3. The mechanism, which may stand behind such behavior, is the hexagonal crystal field, which, although it does not play much of a role for the spin aligning itself, is high enough to enforce the distribution of A, B, C, and D centers at low temperatures. Even at $T=10$ K [see Fig. 3 (right-hand side)] the experimental data are well described by the model assuming only an A center present in the crystal.

B. Magnetization of $Cd_{1-x}V_xSe$

In the case of $Cd_{1-x}V_xSe$ crystals, anisotropy of magnetization also exists (see Figs.1 and 4) but is much weaker than the anisotropy of $Cd_{1-x}V_xS$. One of the possible explanations is that the population of centers A, though dominating over the populations of B, C, and D, does not monopolize all the centers. The reason for this may be that the hexagonal crystal field of CdSe is weaker than it was for CdS, though it still favors the direction of the c axis. In effect all types of centers contribute to the magnetization. For magnetic field parallel to the c axis the centers B, C, and D are equally populated (direction of $\mathbf{B}$ coincides with the c axis is then a threefold axis for these centers). For $\mathbf{B}\perp c$ the population of centers B, C, and D should differ, since magnetic field lowers the symmetry of the problem. At least one of these three centers is then privileged. Nevertheless, the magnetization calculated as a function of the angle around the c axis (for

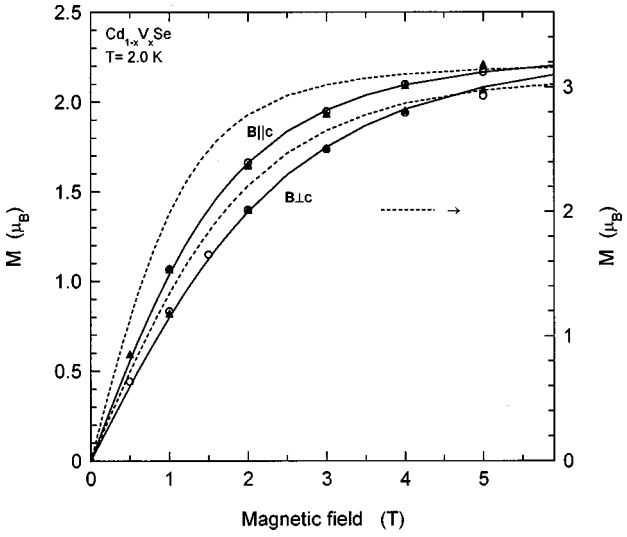

FIG. 4. Calculated magnetization curves (in Bohr magnetons) for $Cd_{1-x}V_xSe$ together with the experimental data for $\mathbf{B}\|c$ and $\mathbf{B}\perp c$ at $T=2.0$ K. The data were corrected for the diamagnetic contribution of the CdSe lattice $\chi^{d}_{CdSe}=-3.34\times10^{-7}$ $e$mu/g (Ref. 17) and then divided by the molar fraction of vanadium x to obtain the Bohr magneton units. Solid lines represent the calculations or all four types of V^{2+} centers present in the crystal (center with the distortion axis parallel to the c axis appear twice more often than any of the other centers in the crystal). Dashed lines show the magnetization calculated assuming only one center (as for $Cd_{1-x}V_xS$) but with the spin-orbit parameter of V^{2+} ion: $\lambda=-20$ cm^{-1} (the right-hand scale).

$\mathbf{B}\perp c$) showed that it depends on this angle very weakly in the equilibrium model defined by Eq. (2) (differences do not exceed 3% of the magnitude of magnetization). A very good description of the experimental magnetization is obtained for $\alpha=2$, which means that population of V^{2+} centers distorted along the c axis is doubled with respect to the other centers. This may result from the fact that in $Cd_{1-x}V_xSe$ the hexagonal crystal field is weaker than in CdS, leading to a more uniform distribution of the different Jahn-Teller centers than for CdS ($\alpha\rightarrow\infty$). Adopting $\alpha=2$ and using all the other parameters (including λ) the same as for CdS one obtains results shown in Fig. 4.

The second possible explanation of the weaker anisotropy of $Cd_{1-x}V_xSe$ is that the V^{2+} ion is surrounded by Se anions, for which the sign of the spin-orbit coupling is opposite to the sign of the free V^{2+} ion. The selenium ligands have stronger spin-orbit coupling than sulfur ligands affecting V^{2+} in $Cd_{1-x}V_xS$ crystals. Therefore if the admixture of the ligands' wave functions to the V^{2+} states is considerable, it may even reverse the sign of the spin-orbit constant λ of the V^{2+} ion [we recall that a similar situation occurs for the Cr^{2+} ion in ZnTe, where a low-energy diagram is inverted with respect to the Cr^{2+} ion in ZnSe (Refs. 8 and 9). Therefore to decrease the magnetic anisotropy one should decrease the magnitude of the spin-orbit coupling of V^{2+}. This would result in a decrease of the splitting of the lowest energy levels of V^{2+} [see Figs. 2(b) and 2(c)]. However, although lowering the spin-orbit parameter weakens the anisotropy, it also results in the crossing of the magnetization for $\mathbf{B}\|c$ and $\mathbf{B}\perp c$ at about 5 T, which is not observed in the experiment. Only if one changes the sign of the spin-orbit constant λ (and, in effect, admixture of the orbital momentum to the magnetization) the magnetization does not cross and have the proper anisotropy. This may be achieved for $\lambda\approx-20\ \mathrm{cm}^{-1}$. However, the calculated magnetization for both $\mathbf{B}\|c$ and $\mathbf{B}\perp c$ saturates faster with the magnetic field than the experimental data (compare the dotted curve with the experimental points in Fig. 4).

These facts led us to the conclusion that the driving mechanism of the weaker magnetic anisotropy of $Cd_{1-x}V_xSe$ than for $Cd_{1-x}V_xS$ is the contribution of the Jahn-Teller centers with the distortion axes not parallel to the hexagonal axis. The spin-orbit coupling of V^{2+} ion, in this case, can be assumed to be of similar magnitude for both $Cd_{1-x}V_xSe$ and $Cd_{1-x}V_xS$ (we recall that the spin-orbit parameters for the Cr^{2+} ion were similar for $Cd_{1-x}Cr_xS$ and $Cd_{1-x}Cr_xSe$ crystals[8]).

IV. CONCLUSIONS

The anisotropy of magnetization in the wurtzite crystals $Cd_{1-x}V_xS$ and $Cd_{1-x}V_xSe$ was studied for the magnetic field applied parallel or perpendicular to the hexagonal axis c, which is an easy axis of the macroscopic magnetization. Within the crystal-field model, strong anisotropy observed for $Cd_{1-x}V_xS$ and $Cd_{1-x}V_xSe$ results from hexagonal crystal-field-induced redistribution of the different V^{2+} centers. In the case of CdS, hexagonal crystal field is so strong that practically all the centers orient their Jahn-Teller distortion along the crystal hexagonal axis. On the other hand, for CdSe hexagonal crystal field is weaker, so all the types of centers exist, but the population of the centers distorted along the c axis is doubled with respect to any others.

ACKNOWLEDGMENT

We acknowledge partial financial support from The State Committee of Scientific Research (Poland), in particular, under Grant No. 2 P03B 042 12.

[1] *Diluted Magnetic Semiconductors*, edited by J.K. Furdyna and J. Kossut, Semiconductors and Semimetals Vol. 25 (Academic Press, New York, 1988); *Diluted Magnetic Semiconductors*, edited by M. Balkanski, M. Averous (Plenum, New York, 1991); J. Kossut and W. Dobrowolski, in *Handbook of Magnetic Materials*, edited by K.H.J. Buschow (North-Holland, Amsterdam, 1993), Vol. 7, p. 231.

[2] J. Blinowski, P. Kacman, and H. Przybylińska, Solid State Commun. **79**, 1021 (1991).

[3] J. Blinowski and P. Kacman, Phys. Rev. B **46**, 12 298 (1992); J. Blinowski, P. Kacman, and J.A. Majewski, Acta Phys. Pol. A **88**, 683 (1995); J. Cryst. Growth **159**, 973 (1996).

[4] W. Mac, Nguyen The Khoi, A. Twardowski, J.A. Gaj, and M. Demianiuk, Phys. Rev. Lett. **71**, 2327 (1993).

[5] W. Mac, A. Twardowski, and M. Demianiuk, Phys. Rev. B **54**, 5528 (1996).

[6] J.T. Vallin, G.A. Slack, S. Roberts, and A.E. Hughes, Phys. Rev. B **2**, 4313 (1970).

[7] J.T. Vallin and G.D. Watkins, Phys. Rev. B **9**, 2051 (1974).

[8] W. Mac, A. Twardowski, P.J.T. Eggenkamp, H.J.M. Swagten, Y. Shapira, and M. Demianiuk, Phys. Rev. B **50**, 14 144 (1994).

[9] G.H. McCabe, Y. Shapira, V. Bindilatti, N.F. Oliveira, A. Twardowski, W. Mac, E.J. McNiff, and M. Demianiuk, Solid State Commun. **95**, 841 (1995).

[10] M. Herbich, W. Mac, A. Twardowski, K. Ando, Y. Shapira, and M. Demianiuk, Phys. Rev. B **58**, 1912 (1998).

[11] J. Schneider, B. Dischler, and A. Rauber, Solid State Commun. **5**, 606 (1967).

[12] R. Krevet, A. Twardowski, M. von Ortenberg, W. Mac, and M. Demianiuk, Solid State Commun. **87**, 709 (1993).

[13] W. Mac, A. Twardowski, M.E.J. Boonman, A. Wittlin, R. Krevet, M. von Ortenberg, and M. Demianiuk, Physica B (Amsterdam) **211**, 384 (1995).

[14] A. Abragam and B. Bleaney, *Electron Paramagnetic Resonance of Transition Metal Ions* (Clarendon, Oxford, 1970).

[15] R. Pappalardo and R.E. Dietz, Phys. Rev. **123**, 1188 (1961).

[16] Le Manh Hoang and J.M. Baranowski, Phys. Status Solidi B **84**, 361 (1977).

[17] M.E. Lines and J.V. Waszczak, J. Appl. Phys. **48**, 1395 (1977).